Comparison of high-power energy storage devices for frequency regulation application (Performance, cost, size, and lifetime)

Soltani, Mahdi; Ibrahim, Tarek Mahmoud Samy Mostafa; Stroe, Ana-Irina; Stroe, Daniel-Ioan

Published in:
Proceedings of IECON 2022 – 48th Annual Conference of the IEEE Industrial Electronics Society, 2022

Publication date:
2022

Document Version
Accepted author manuscript, peer reviewed version

Comparison of high-power energy storage devices for frequency regulation application (Performance, cost, size, and lifetime)

Mahdi Soltani
Energy
Aalborg University
Aalborg, Denmark
maso@energy.aau.dk

Tarek Ibrahim
Energy
Aalborg University
Aalborg, Denmark
taib@et.aau.dk

Ana-Irina Stroe
KK Wind Solutions A/S
Ikast, Denmark
anstr@kkwindsolutions.com

Daniel-Ioan Stroe
Energy
Aalborg University
Aalborg, Denmark
dis@energy.aau.dk

***Abstract*—The penetration of renewable energy sources (RES) has caused some challenges for grid operation, including frequency variation, low power quality, and reliability issues. These challenges can be mitigated with the help of battery energy storage systems (BESS) which are characterized by long lifetime and high-power capability. Among the different types of high-power storage devices, lithium titanate oxide (LTO) batteries and lithium-ion capacitor (LIC) cells attract more attention. The performance behavior, the total cost of the battery system, and the system's size are some other criteria for cell selection. This research compares the performance behavior of an LTO battery type for this application with two LIC type storage system at positive and negative temperatures and also considers the system size, cost, and lifetime of the BESS. The result proves that LICs are better candidates for low and high temperature applications in terms of energy efficiency and capacity drop. However, in terms of cost and size, the high-energy LTO cells are a better selection.**

Keywords— frequency regulation application, high-power storage device, Lithium titanate oxide, Lithium-Ion capacitor, low and high temperature, capacity, energy efficiency, internal resistance.

I. INTRODUCTION

In recent years, the demand for high-power (HP) energy storage systems (ESSs) has grown rapidly. Mega fast chargers [1], hybrid energy storage systems [2], high-power electric mobility (trains, ships, and heavy-duty vehicles) [3], and frequency regulation [4] are some examples of high-power ESS applications. Depending on the application, different requirements for high-power ESS arise. Some of the key requirements of the high-power ESS for frequency regulation application are the performance stability [5] at low and high temperatures, and long cycle life. Among the different types of high-power ESS, lithium-titanate-oxide (LTO) cells and lithium-ion capacitors (LIC) attract more attention due to their higher energy density compared to the electrochemical double-layer capacitors (EDLCs) [6], [7]. LTOs also are characterized as long lifetime LIB due to their low operating voltage, which limits the SEI formation and the cell's degradation [8] [9]. Moreover, the dendrite-formation at low temperatures during fast charging applications is negligible [10]. LIC, as a hybrid technology is composed of a LIB anode and an ELDC cathode [11]. LIC has a longer cycle life and higher power-capability compared to the LIBs and a higher energy density compared to the EDLCs [12]. The negative electrode of LIC is composed of graphite or LTO material and the positive electrode is activated carbon (AC). Depending on the material used in LICs, different performance can be achieved at low and high temperature.

Comprehensive research is required to select the best device for frequency regulation application from the above-mentioned high-power energy storage system. To the best of the authors' knowledge, such research has not been presented in the literature yet.

In this research paper, a grid-scale fast response BESS with a 1 MW/250 kWh battery used for frequency regulation application in Hawaii's power system is referenced for battery system design [13]. For this purpose, battery systems composed of different high power storage systems (a LTO and two LICs) are designed, dimensioned, and compared from cost, lifetime, efficiency, and performance perspective.

II. HAWAII POWER SYSTEM AND FREQUENCY REGULATION ALGORITHM

The Hawaii island power system comprises 73 MW of PV, 31 MW of wind, 38 MW of Geothermal, and 16 MW of run of river hydro power generation with a power system peak of approximately 190 MW as reported in March 2016 [14]. The Hawai'i Natural Energy Institute (HNEI), at the University of Hawaii has conducted research to evaluate the advantages of grid-scale BESS for frequency regulation applications. To this purpose, three grid-scale fast response BESS (1 MW/250 kWh) have been installed on the Hawaiian Islands grids at the transmission and distribution levels and a closed loop control algorithm has been used to maximize the grid support and to extend the lifetime of BESS by reducing the number of cycles of the battery system.

In order to develop a frequency response algorithm, a Power-frequency (P-f) curve has been configured with a deadband of various widths and with various proportional gains, i.e., the slope of the P-f curve in MW/Hz. The result of the P-f curve has been used to maintain a target state-of-charge (SOC). The frequency response algorithm was tested within a simple grid model. The proportional gain (slope of the P-f curve) of 30 MW/Hz, or more was found to be sufficient to significantly reduce frequency variability. A higher proportional gain (40 MW/Hz) with no deadband leads to a

greater grid benefit. However, it causes a substantial burden on the BESS because of more energy throughput (cycling) and a more temperature increase.

III. Experimental Setup

A. Investigated High Power Energy Storage Devices

Three high-power storage devices are studied and used for ESS design for frequency regulation application. The specifications of high power storage devices under test are summarized in Table I. The LTO battery in this study is composed of an LTO anode and an NMC cathode material [15] with a long lifecycle of more than 16000 full equivalent cycles (FECs) and a wide operating temperature (-40 to +50 ℃). The LIC2100 F in this study is composed of a graphite anode and an activated-carbon (AC) cathode with an extremely long lifetime (> 300,000 FEC) and high power density. The wide operating temperature (-30 to +70℃) and high continuous current rate (53C) are some of the other characteristics. It should be noted that the lifecycle of the LIC compared to the LTO is much higher if similar current rates are referenced for comparison. The LIC9000 F stands between LIC2100 F and LTO cell in terms of operating temperature (-20 to +65℃), specific energy (48.8), and lifetime. However, the lifetime data presented by the manufacturer is for the 1C current rate, which is not comparable with LIC2100 F. The lifetime study of LIC2100 F and LIC9000 F in different operating conditions are ongoing in our research group. The price of each device has been presented proportional to the LTO 50 Ah cells used by HNEI.

TABLE I. Characteristics of the Investigated Devices

Properties	Investigated HP ESS		
	LTO 13 Ah	***LIC 9000F***	***LIC 2100 F***
Nominal capacity (Ah)	13	4	0.93
Voltage (nominal voltage) (V)	1.5-2.9 (2.26)	2.5-4 (3.2)	2.2 -3.8 (3)
Maximum current (continuous) (A)	130	30	50
Operating temperature (℃)	-40 to +50	-20 to +65	-30 to +70
End of life (FEC)	> 16000 at 25 ℃ , 100% cycle depth (CD), 2C/2C	> 25000 at 25 ℃ , 100% CD, 1C/1C	> 300,000 at 25 ℃, 100% CD, 50C/50C
End of life (year)	> 25	5	Not given by the manufacturer
DC-IR (mΩ)	1.5 at 25°C,	6 at 25°C	6.2 at 25°C, 10A
Specific energy (Wh/kg)	74	48.8	24
Energy density (Wh/L)	146	77.7	40
Specific power (kW/kg)	1.611 at 260 A	1.1 at 90A	4 at 200A
Power density (kW/L)	3.180 at 260 A	1.748 at 90A	6 at 200A
Volume (L)	0.207	0.164	0.11
Weight (kg)	0.167	0.262	0.11
Cost (%)	22	9.5	13.2

B. Test Equipment

The performance tests have been conducted using a Digatron battery test station. During all the experiments, the cells were placed in Memmert temperature chambers in order to ensure stable and reliable temperature. The test set-up is shown in Fig. 1.

Fig. 1. Battery test setup. Digatron BTS 600 (right), Memmert UFP 600 temperature chamber containig LIC battery(left).

IV. Test Conditions and Procedures

In order to compare the performance behavior of the selected devices, the capacity, resistance, and energy efficiency characteristics are measured according to IEC 62660-1 for LIBs [16], IEC 62391-1 for EDLCs [17], and IEC 62813-1 for LICs [18].

A. Preconditioning

Before starting characterization, the cell is conditioned by performing a certain number of charge/discharge cycles in order to ensure stabilisation of the battery cell. The cell is considered preconditioned if the capacity variation between two consecutive cycles is less than 3% during five cycles.

B. Capacity

The capacity test has been performed at different temperatures and current rates. It consists of a CC/CV charge at a rated value followed with a CC discharge at different currents and temperatures given in Table II.

TABLE II. Capacity Test Conditions

Properties	Investigated HP ESS		
	LTO 13 Ah	***LIC 9000F***	***LIC 2100 F***
Test C-rates	0.25, 0.5, 1, 2, 3, 4, 7, 9	0.5, 1, 2, 2.5, 5, 7.5	0.1, 1, 5, 10, 20, 30, 40, 50, 53
Test temperature	-10, -5, 0, 5, 15, 25, 35, 45	-10, -5, 0, 5, 15, 25, 35, 45, 55	-10, 0, 10, 25, 30, 40, 50, 60

C. DC Internal Resistance

The DC internal resistance (DC-IR) is measured according to the IEC 62660-1 for LIBs, and IEC 62813-1 for LICs at different temperatures, as shown in Table II. For the LTO cell, a 10 s charge/discharge pulse at 50% SOC for different temperatures is used. The voltage variation ratio to the current during the pulse is used for DC-IR calculation. For LICs, the immediate voltage drop after pulse start divided by the test current is used to calculate the DC-IR. The rapid voltage drop is calculated according to the IEC 62813-1 and shown in Fig. 2. For DC-IR measurement, mostly the manufacturer recommends the test current, otherwise it is calculated as explained in (1). For LIC 2100 F, the test current

recommended by the manufacturer is 10 A and is used for DC-IR determination. For the LIC 9000 F, the current has been calculated by (1) which is equal to 5 A.

$$I = \frac{1}{30R_N} \times \sqrt{1 + \frac{27}{5C_N R_N + 1} - \frac{26}{10C_N R_N + 1}} \quad (1)$$

Where I is the charging/discharging current, R_N is the nominal internal resistance of the LIC under test (Ω), and C_N is the nominal capacitance (F). It should be noted that the current calculated above is meant to limit the resultant measurement error of internal resistance within ± 3 %.

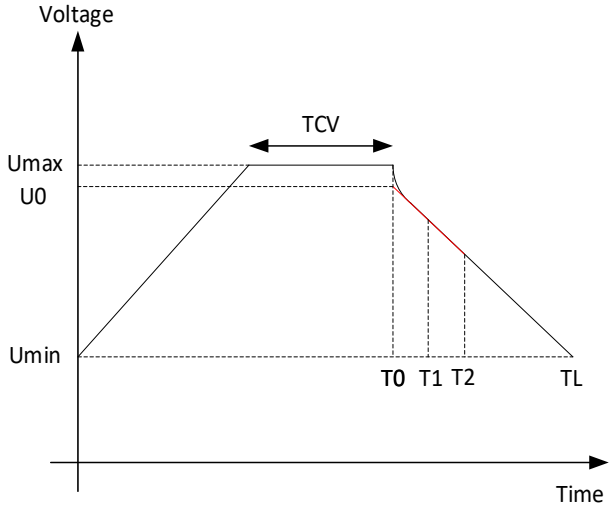

Fig. 2. Internal resistance and capacitance determination methodology

The rapid voltage drop is defined as (U_{max}-U_0) where U_0 is the calculated voltage at the intersection of vertical line at T_0 and the straight line that connects points T_1 and T_2 as shown in Fig.2. In this figure, T_0 is the discharge start time, T_1 is calculation start time (C_N.R_N), T_2 is calculation end time (2.C_N.R_N), T_L is the minimum cut-off voltage time, T_{CV} is the CV charge duration, U_R is maximum rated voltage, U_L is the minimum cut-off voltage, and U_0 is the instant drop voltage at discharge start time. The T_1 and T_2 are calculated 13.2 s and 26.4 s for LIC2100 F and 54 and 108 s for LIC9000 F.

D. Energy efficiency

Energy efficiency is the ratio of discharge energy to the charge energy. According to the IEC 62660-1 standard, the charge energy is measured through a CC-CV charge process at different temperatures for different current rates performed on a fully discharged cell through a rated current discharge. The cell is then discharged with a similar current to the minimum cut-off voltage at the same temperature.

V. Result and Discussion

A. Capacity test result

The capacity test result for all high-power ESSs in this research has been presented in Fig.3 to Fig.5 as a function of C-rate for different temperatures. For all high-power ESSs, the capacity decreases with the decrease of temperature and the increase of C-rate. For a similar current and test temperature, i.e., 7C and -10°C, the LIC2100 F has the highest normalized capacity. The normalized capacity is the ratio of the test capacity to the nominal capacity measured at the rated current and room temperature.

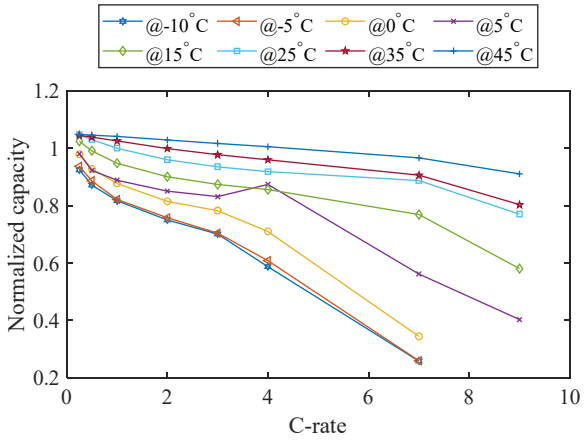

Fig. 3. Capacity variation as a function of C-rate for different temperatures for LTO cell.

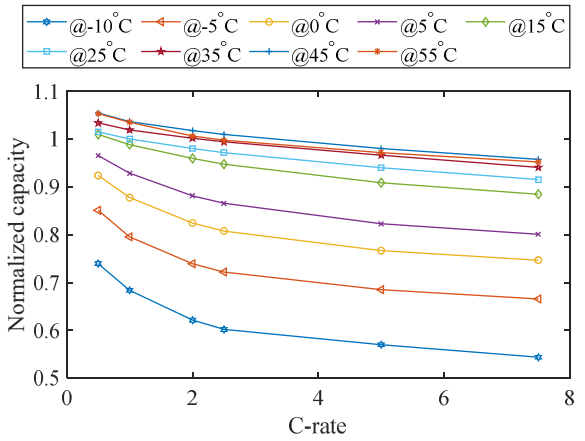

Fig. 4. Capacity variation as a function of C-rate for different temperatures for LIC 9000F cell.

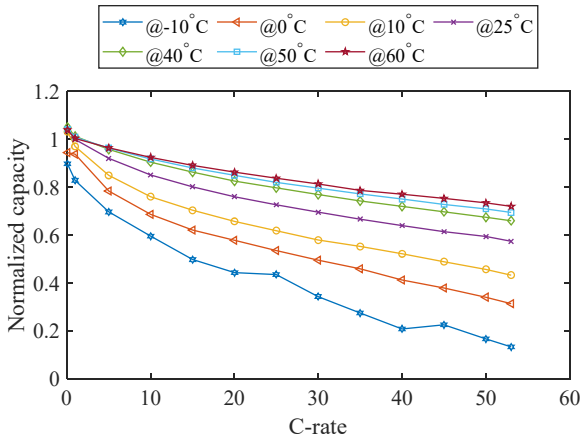

Fig. 5. Capacity variation as a function of C-rate for different temperatures for LIC 2100F cell.

B. DC resistacne

The DC internal resistance results for all high-power ESSs are presented in Fig.6 for different temperatures. For LIC9000 F, the internal resistance at low temperature is 20 times higher than the value at 25°C, while for LIC2100 F and LTO cell, the

resistance at low temperature is four times higher than 25°C. As shown in Fig.6, LTO has a lower internal resistance than the LICs in this research and consequently has a lower ohmic loss. It is also seen from Fig.6 that the internal resistance of the LIC9000 increases at high and low temperatures compared to DC-IR at 25°C while for LIC2100 F and LTO cells, the internal resistance decreases with the increase of temperature. The difference in internal resistance behaviour can be due to the different electrode materials used in these 3 devices.

C. *Energy efficiency*

Energy efficiency is the most important factor in the grid connected application because it is directly translated into the final cost of the energy supplied. Moreover, an efficient ESS reduces the power loss during the charge/discharge process and generates less heat during operation. Having less heat generated inside the storage system requires less cooling power for heat dissipation. Finally, a low heat generation inside the storage system will extend the lifetime of the battery system, which further reduces the supplied energy cost. The energy efficiency of the three HP storage devices has been presented in Fig. 7. The LIC2100 F presents the highest energy efficiency at all test temperatures for 1C current rates. The maximum efficiency for LIC2100 F, LIC9000 F and LTO are 97.6%, 90.4% and 87.7% respectively. Energy efficiency decreases at high currents, and low temperatures as shown in Fig. 8 for LIC2100 F. The lowest energy efficiency is seen at 53C and -10℃, which is 10.4%.

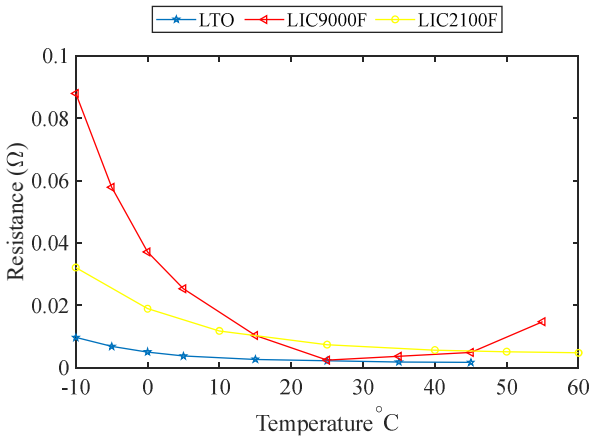

Fig. 6. Comparison of internal resistance variation as a function of temperature at 50% SOC and 1C current.

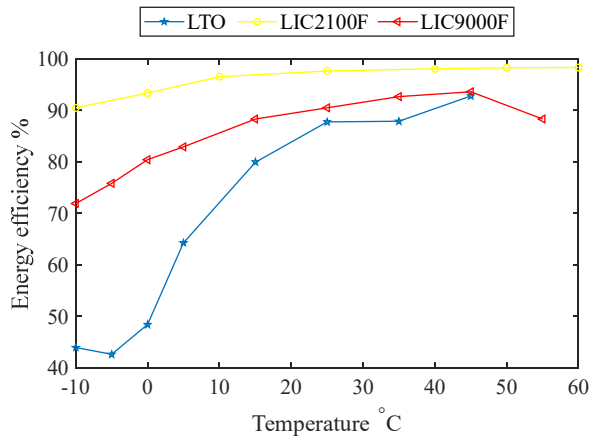

Fig. 7. Comparison of energy efficiency variation as a function of temperature at 1C.

TABLE III. BESS SPECIFICATION DESIGNED BY HNEI

Source	Specification
Datasheet (cell level)	115 W, 115 Wh, 50 Ah, 2.8-1.5 V, 2.3 Vave, 60 Wh/kg, 287.5 W/kg, 11C (max), 16000 FEC, 1 unit price, 1.6 kg

TABLE IV. SUMMARY OF DAILY USAGE

Daily usage (cell)	Maximum	average
power	1.1MW (3.5P)	170 kW (P/2)
current	1.25 kA (3C)	200A (C/2)
energy	5 kWh	1.95 kWh
capacity	6000 Ah	2000 Ah
temperature	55°C	35°C
number of full cycles per day	17	5

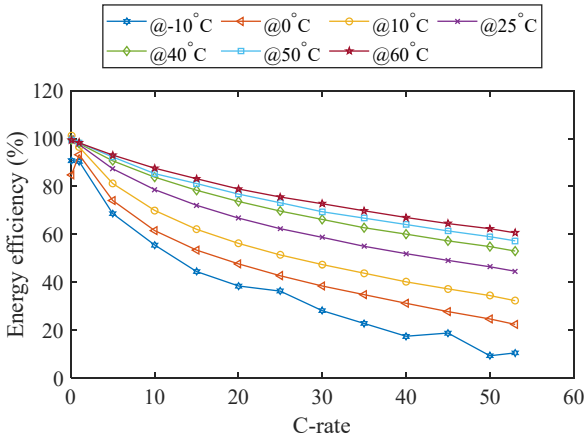

Fig. 8. Energy efficiency variation as a function of C-rate for different temperature for LIC2100 F.

VI. BATTERY STORAGE SYSTEM DESIGN

The characterization result of the three HP storage devices reveals that the LIC2100 F is the best candidate among the selected devices for the frequency regulation application in terms of performance and energy efficiency. Moreover, the capacity and internal resistance of this device in different operating temperature are less impacted by the extreme temperature conditions; however, the system size, cost, and lifetime have to be considered for a proper energy storage system's design. The lifetime of LIC2100 F, as shown in Table I., is more than 300.000 cycles with a 50C/50C cycling profile which proves the compatibility of this device for numerous charge/discharge cycles. A higher lifetime is expected at lower C-rates which is under investigation in our research lab.

The provided information in Table III and Table IV is used to design an ESS in this research paper.

The existing BESS designed and installed by HNEI in this project comprises 384 battery modules in series connection, each with seven 2.3 V, 50 Ah LTO cells connected in parallel. The cells specification and the daily usage information recorded in 3 years are shown in Table III and Table IV respectively.

The average voltage of the BESS designed by HNEI is 884 V (576-1075 V) which is used to calculate the number of cells in series connection in the designed battery storage system (cells in serries connection = 884/Vcell) where Vcell is the average voltage of each cell. The required energy (250 kWh) is used to calculate the total number of cells in the ESS and

later is used to calculate the number of parallel branches (number of cells = 250 kWh/(0.8×Ecell), where Ecell is the energy of cell and 80% is the end-of-life (EOL) criterium. The maximum deliverable power by the ESS is (0.5× Pcell × Nparallel), where 50% is the existing power at the EOL, Pcell is the nominal power of the selected device, and Nparallel is the number of parallel branches. Considering a 100% increase in internal resistance at the EOL, the deliverable power is calculated at 50% of the initial power at the beginning of life (BOL). Finally, the mass, volume, and cost of the ESS are known by having the total number of cells. The calculation result for the three selected energy storage devices is given in Table V. As can be seen in this table, the best device for this application in terms of weight, volume, and initial investment is the LTO 13 Ah cell which can be explained with its higher energy density. In terms of cycle life, the LICs show a longer cycle life than the LTO cells; however, the cycle life and calendar life together determine the lifetime of the ESS. Due to a higher potential of the LIC cells compared to the LTO cells, the number of cells in series connection is lower than the LTO storage system; however, the total number of cells is higher for LIC cells due to their lower energy density compared to the LTOs. The maximum continuous power is determined by the number of parallel branches and the maximum continuous current that each device can provide. The maximum continuous current for the LIC2100 F is the highest value (17.69 kA). Considering that only 50% of the power can be provided by the energy storage system at the end of life, the current provided by the LIC2100 F is far above the requested current in this application, which is 1250 A as shown in Table IV. This can be considered as over design, which increases the cost of the ESS. By using the LIC2100 F storage device in this application, a different frequency response algorithm with a higher proportional gain (i.e., 40 MW/Hz) with no deadband can be selected for a more significant grid benefit without negative impact on lifetime (cycle life) and temperature increase, however, this is highly dependent on the frequency regulation scheme of the target country.

TABLE V. THE ESS DESIGNED IN THIS RESEARCH PAPER

specification of the ESS	**Different ESS**			
	LTO 50Ah (HNEI)	***LTO 13Ah***	***LIC 9000F***	***LIC 2100 F***
Continuous maximum current (kA)	3.85	3.85	2.88	17.69
Average voltage (V)	884	884	884	884
Number of cells in series	384	392	277	295
Number of parallel branches	7	27	103	380
Total number of cells	2,688	10,522	28,410	112,008
Available power at BOL (MW)	3.4	3.4	2.54	15.6
Weight (kg)	4,300	1,757	7,443	12320
Volume (L)	-	2,179	4,660	12,320
Initial investment (%)	100	86.3	101	551
cyclelife (year)	8.76	8.76	13.69	164

The ESS needs to be replaced with new cells after some years, depending on the expected cycle life/calendar life of the selected device. The total cost consists of the initial investment plus the maintenance/operation cost. The total cost has been compared in Fig.9 for different energy storage devices in this research paper. Both the calendar and cycle life have been considered for the cost calculation. The manufacturer has not provided the calendar life of LIC2100 F cell; however, the end of life for a cell with similar technology has been reported as more than 15 years [19]. The end of life of this device, according to the number of cycles per day given in Table IV (5 FEC/day), is 164 years. Therefore, the calendar life is used to calculate the number of replacements and the total cost. For LIC9000 F, the cycle life is 13.69 years as shown in Table V. However, the calendar life is only five years therefore, every five years the initial cost is repeated. For the LTO 50 Ah cell and the LTO 13 Ah cell, the cycle life is shorter than the calendar life; therefore, the cycle life is used to calculate the total cost of operation.

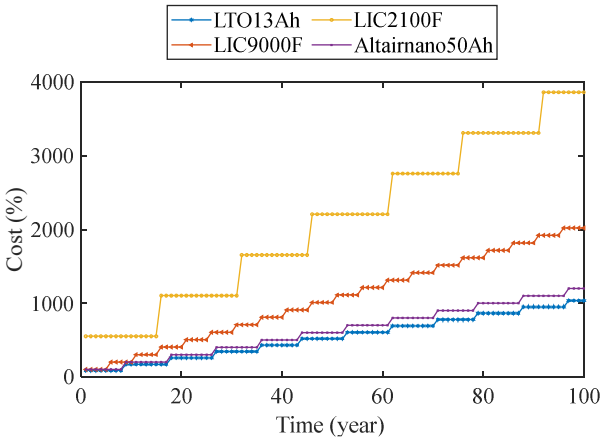

Fig. 9. Cost estimation for different storage devices as a function of operating time

As can be seen in Fig.9 for both the LICs, the total cost is much higher than the LTO cells due to their low energy density and high initial cost. Although for LIC2100F, the number of replacements in 100 years is calculated six times however, due to an increased initial investment and also due to the replacement cost of the LICs, this ESS is turned out to be very costly for this application. For the LIC9100 F, the initial investment is close to the initial investment of the LTO cell selected by HNEI; however, due to a short calendar life, despite its higher cycle life, the number of replacements is higher, which therefore increases the total cost of the ESS. In terms of reliability and maintenance, the LIC2100 F is the best option as it only requires six times of replacement and fewer safety issues, according to the literature [20].

VII. CONCLUSION

In this research, the performance behavior of 3 high-power/high-energy storage devices at the positive and negative temperatures and high currents have been studied to replace a practical storage system designed by HNEI for the Hawaii island. It was found that the LIC2100 F has the highest energy efficiency at all test temperatures for 1C current rates. The maximum efficiency for LIC2100 F, LIC9000 F, and LTO are 97.6%, 90.4%, and 87.7%, respectively. Later, energy storage systems using the selected devices have been designed and compared in terms of cost, size, and lifetime. It was found that the LIC2100 F device has the longest lifetime considering both the calendar life and cycle life; however, in terms of cost and size, the LTO 13 Ah device is the best option.

ACKNOWLEDGMENT

This research is part of the SENSE – Sustainable Energy Systems, which is supported by the Energy Technology Development and Demonstration program (EUDP), Denmark, under the grant no. 64019-00114.

REFERENCES

[1] J. Groot, M. Swierczynski, A. I. Stan, and S. K. Kær, "On the complex ageing characteristics of high-power LiFePO4/graphite battery cells cycled with high charge and discharge currents," J. Power Sources, vol. 286, pp. 475–487, 2015, doi: 10.1016/j.jpowsour.2015.04.001.

[2] M. Soltani et al., "Hybrid battery/lithium-ion capacitor energy storage system for a pure electric bus for an urban transportation application," Appl. Sci., vol. 8, no. 7, 2018, doi: 10.3390/app8071176.

[3] T. Kalogiannis et al., "Comparative Study on Parameter Identification Methods for Dual-Polarization Lithium-Ion Equivalent Circuit Model," Energies, vol. 12, no. 21, p. 4031, 2019, doi: 10.3390/en12214031.

[4] M. Swierczynski, D. I. Stroe, A. I. Stan, R. Teodorescu, and D. U. Sauer, "Selection and performance-degradation modeling of limo2/li 4ti5o12 and lifepo4/c battery cells as suitable energy storage systems for grid integration with wind power plants: An example for the primary frequency regulation service," IEEE Trans. Sustain. Energy, vol. 5, no. 1, pp. 90–101, 2014, doi: 10.1109/TSTE.2013.2273989.

[5] K. Stein, M. Tun, K. Musser, and R. Rocheleau, "Evaluation of a 1 MW, 250 kW-hr battery energy storage system for grid services for the island of Hawaii," Energies, vol. 11, no. 12, 2018, doi: 10.3390/en11123367.

[6] T. Nemeth, P. Schröer, M. Kuipers, and D. U. Sauer, "Lithium titanate oxide battery cells for high-power automotive applications – Electro-thermal properties, aging behavior and cost considerations," J. Energy Storage, vol. 31, no. April, p. 101656, 2020, doi: 10.1016/j.est.2020.101656.

[7] D. Stroe, M. Swierczynski, A. I. Stan, and R. Teodorescu, "Accelerated lifetime testing methodology for lifetime estimation of Lithium-ion batteries used in augmented wind power plants," 2013 IEEE Energy Convers. Congr. Expo. ECCE 2013, vol. 50, no. 6, pp. 690–698, 2013, doi: 10.1109/ECCE.2013.6646769.

[8] G. Xu, P. Han, S. Dong, H. Liu, G. Cui, and L. Chen, "Li4Ti5O12-based energy conversion and storage systems: Status and prospects," Coord. Chem. Rev., vol. 343, pp. 139–184, 2017, doi: 10.1016/j.ccr.2017.05.006.

[9] A. I. Stroe, J. Meng, D. I. Stroe, M. Świerczyński, R. Teodorescu, and S. K. Kær, "Influence of battery parametric uncertainties on the state-of-charge estimation of lithium titanate oxide-based batteries," Energies, vol. 11, no. 4, 2018, doi: 10.3390/en11040795.

[10] B. P. Matadi et al., "Effects of Biphenyl Polymerization on Lithium Deposition in Commercial Graphite/NMC Lithium-Ion Pouch-Cells during Calendar Aging at High Temperature," J. Electrochem. Soc., vol. 164, no. 6, pp. A1089–A1097, 2017, doi: 10.1149/2.0631706jes.

[11] M. Soltani and S. H. Beheshti, "A comprehensive review of lithium ion capacitor: development, modelling, thermal management and applications," J. Energy Storage, vol. 34, no. October 2020, p. 102019, 2021, doi: 10.1016/j.est.2020.102019.

[12] M. Soltani, L. De Sutter, J. Ronsmans, and J. Van Mierlo, "A high current electro-thermal model for lithium-ion capacitor technology in a wide temperature range," J. Energy Storage, vol. 31, no. January, p. 101624, 2020, doi: 10.1016/j.est.2020.101624.

[13] K. Stein, M. Tun, M. Matsuura, and R. Rocheleau, "Characterization of a fast battery energy storage system for primary frequency response," Energies, vol. 11, no. 12, pp. 1–12, 2018, doi: 10.3390/en11123358.

[14] M. Dubarry, A. Devie, K. Stein, M. Tun, M. Matsuura, and R. Rocheleau, "Battery Energy Storage System battery durability and reliability under electric utility grid operations: Analysis of 3 years of real usage," J. Power Sources, vol. 338, no. March 2016, pp. 65–73, 2017, doi: 10.1016/j.jpowsour.2016.11.034.

[15] A. I. Stroe, D. L. Stroe, V. Knap, M. Swierczynski, and R. Teodorescu, "Accelerated Lifetime Testing of High Power Lithium Titanate Oxide Batteries," 2018 IEEE Energy Convers. Congr. Expo. ECCE 2018, pp. 3857–3863, 2018, doi: 10.1109/ECCE.2018.8557416.

[16] IEC 62660-1, Secondary lithium-ion cells for the propulsion of electric road vehicles – Part 1: Performance testing, vol. 43. 2018.

[17] A. Universitetsbibliotek, "Dansk standard Faste elektriske dobbeltlagskondensa- torer til brug i elektrisk og elektronisk udstyr – Del 1 : Generisk specifikation Fixed electric double-layer capacitors for use in electric and electronic equipment – Part 1 : Generic specification," 2020.

[18] INTERNATIONAL ELECTROTECHNICAL COMMISSION, Lithium ion capacitors for use in electric and electronic equipment – Test methods for electrical characteristic (IEC 62813), 1.0., vol. 2016. IEC, 2016.

[19] M. Soltani, J. Ronsmans, and J. Van Mierlo, "Cycle life and calendar life model for lithium-ion capacitor technology in a wide temperature range," J. Energy Storage, vol. 31, no. July, p. 101659, 2020, doi: 10.1016/j.est.2020.101659.

[20] M. Soltani et al., "Three dimensional thermal model development and validation for lithium-ion capacitor module including air-cooling system," Appl. Therm. Eng., vol. 153, no. March, pp. 264–274, 2019, doi: 10.1016/j.applthermaleng.2019.03.023.